BULLETIN OF THE POLISH ACADEMY OF SCIENCES
TECHNICAL SCIENCES, Vol. 61, No. 2, 2013
DOI: 10.2478/bpasts-2013-0050

Comparison of experimental and modelling results of thermal properties in Cu-AlN composite materials

M. CHMIELEWSKI[1]* and W. WEGLEWSKI[2]

[1] Institute of Electronic Materials Technology, 133 Wolczynska St., 01-919 Warsaw, Poland
[2] Institute of Fundamental Technological Research, 5B Pawińskiego St., 02-106 Warsaw, Poland

Abstract. Copper-based composites could be widely used in automotive, electronic or electrical industry due to their very promising thermal properties. In the present paper, Cu-AlN metal matrix composites with ceramic volume fractions between 0.1 and 0.4 were fabricated by hot pressing method in vacuum. Dependence of the coefficient of thermal expansion (CTE) and the thermal conductivity (TC) on the chemical composition of composites has been investigated. The measured values of the thermal expansion coefficient have been compared with the analytical models' predictions. A numerical model based on FEAP 7.5 in 3D space has been used to evaluate the influence of the porosity on the thermal properties (thermal conductivity) of the composite. A fairly good correlation between the FEM results and the experimental measurements has been obtained.

Key words: thermal properties, porosity, copper-based composites.

1. Introduction

Microelectronic circuits require contact with a high thermal conductivity as well as controlled low coefficients of thermal expansion of heat-sink materials to remove the heat generated during their working period [1]. The fulfillment of these requirements by conventional materials is practically impossible. MMCs are most widely used in electronic packaging due to their unique properties combining a high thermal conductivity (due to the metal matrix) and a low coefficient of thermal expansion (due to the ceramic reinforcement). Such combination allows designing new materials with a wide range of thermal properties. Many studies were devoted in the past to the design and fabrication of advanced materials characterized by a very good thermal conductivity, such as Cu-Mo, Cu-Be, Cu-C_f, SiC-Cu, SiC-Al, AlN-Al [2–3] and, more recently, AlN-Cu composite materials [4–8]. The latter material is a particularly attractive candidate for application as a heat dissipation material. Aluminium nitride has advantageous mechanical and electrical properties and a low thermal expansion coefficient (4.0×10^{-6} 1/K) close to that of silicon (2.7×10^{-6} 1/K), which prevents high residual thermal stresses induction [7]. This property is crucial since the failure of electronic devices takes place most frequently due to high residual stresses induced as a result of the mismatch between the thermal expansion coefficients of a substrate and a semiconductor component. The thermal conductivity of polycrystalline aluminium nitride is slightly below 200 W/mK. Copper with a thermal conductivity of about 400 W/mK is used whenever both high thermal and electric conductivities are required, but the application range of this material is limited because of its unsatisfactory mechanical properties, especially at elevated temperatures. Moreover, the high thermal expansion coefficient of copper (16.5×10^{-6} 1/K) may result in considerable residual stresses induction and in thermal dilatation occurring when copper components are subject to substantial temperature variations.

With regard to the fabrication of Cu-AlN composites there are not too many works reported in the literature [8, 9]. The authors of [8] employed a hot pressing method to obtain Cu-AlN composite materials at 1050°C. They used presintered AlN-Y_2O_3 grains (75–150 μm) after the pulverization process. Using higher temperatures is limited by the melting point of copper (1083°C) and lack of wettabillity of aluminium nitride by liquid copper [9]. This disadvantage can be changed by modifying of ceramic substrate by different techniques like: ion implantation or ion beam treatment [10–13]. In [14] the spark plasma sintering (SPS) process was applied to obtain functionally graded materials containing Cu-AlN composite layers.

Some properties of composite materials can be determined using numerical modelling, replacing often cumbersome and costly experimental tests [15]. Modelling was useful for the prediction of the most significant properties in the early stages of the material technology design process. On the other hand, by means of experimental testing one is able to verify the assumptions of proposed theoretical models. Therefore, theoretical modelling and experimental measurements are complementary and help to understand the correlations between the theory and practical aspects of real materials analysis.

The objective of this paper is: (i) to manufacture Cu-AlN metal matrix composite materials using a hot pressing method in vacuum, (ii) to characterise its microstructure and measure thermo-mechanical properties (CTE, TC) depending on the volume fraction of the components, and (iii) to develop and

*e-mail: marcin.chmielewski@itme.edu.pl

verify numerical models capable of predicting the thermal conductivity for the manufactured Cu-AlN composites.

2. Experimental procedure

Copper powder (average grain size 40 μm) with a commercial purity of more than 99.99% was used as the metal matrix. Aluminium nitride particles of a mean size of about 2 μm strengthened the copper matrix. Figure 1 shows the powders used in the experiments.

a)

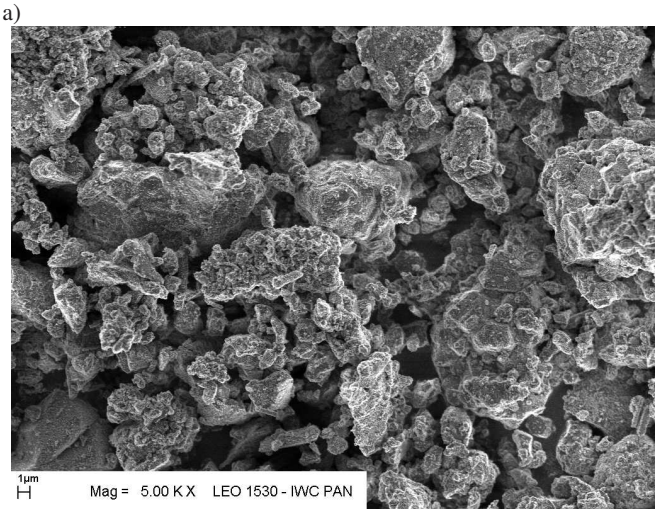

b)

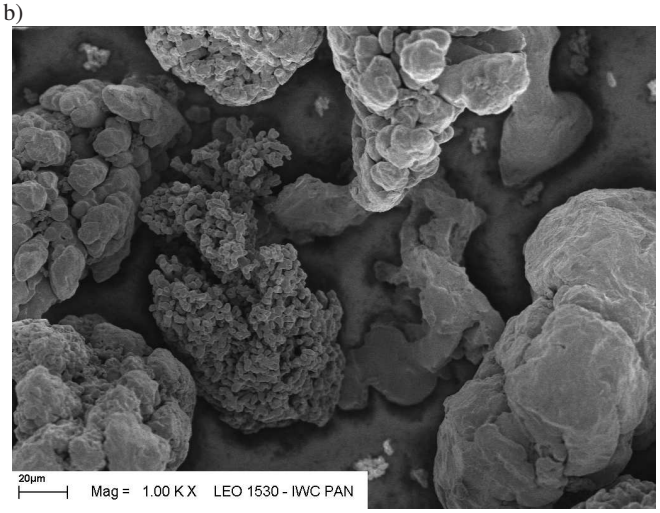

Fig. 1. SEM images of starting materials aluminium nitride (a) and copper powder (b)

The Cu-AlN composite materials with volume fractions of AlN varying from 0.1 to 0.4 were prepared by a powder metallurgy process. The powder mixtures were obtained in a mechanical mixing process using a planetary ball mill (Pulverisette 6, Fritsch) with tungsten carbide balls (∅ 10 mm). The mixing process was conducted in a N_2 atmosphere with the rotational speed of 200 rpm and the time of mixing was 4 h. *Ball–to–powder ratio* (BPR) was approximately 5:1. Presented mixing conditions were selected after the preliminary tests described in papers [16, 17]. The morphology of the obtained powder mixtures is presented in Fig. 2.

a)

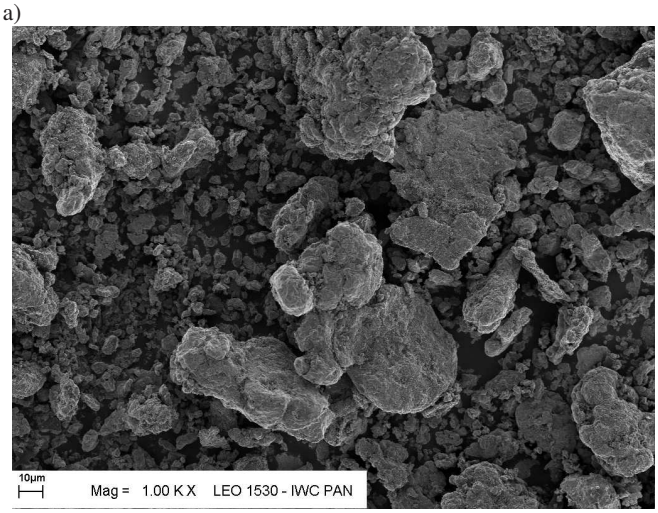

b)

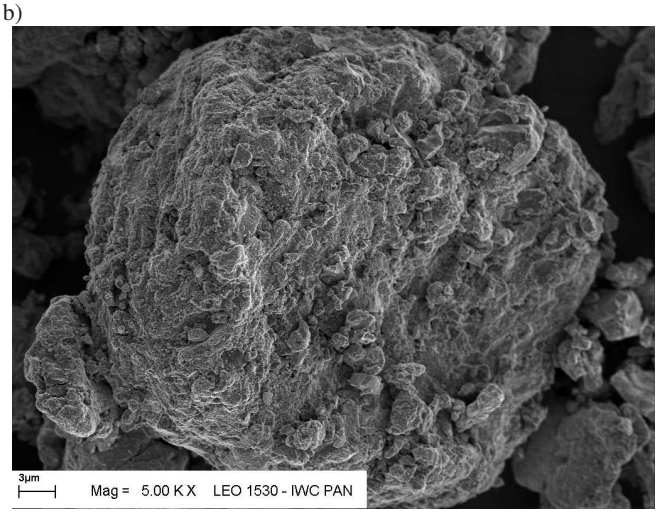

c)

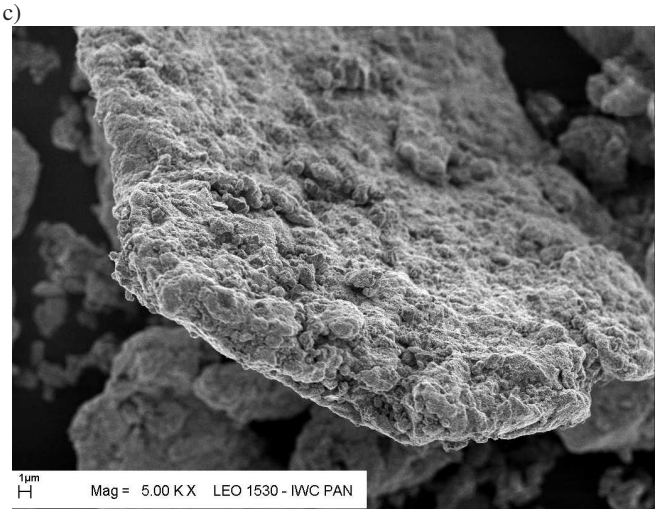

Fig. 2. SEM images of 80Cu-20AlN powder mixtures

Microstructural examinations showed large variations in the size and shape of the obtained powder mixtures. In the case of a higher volume fraction of copper (90–80 vol%) the average grain size of mixtures is about 10 μm after 4-hours of the mixing process. Larger grains can be distinguished (max. 30–40 μm) in the structure of the powder mixtures.

Their shape is rather irregular, but some of them tend to have a spherical form. As a result of the grains breakage as the milling process is continued, sharp edges appear and the grains take flake-like shapes. Aluminium nitride particles are placed on the surface of larger copper grains. Some of them form agglomerates. For higher content of aluminium nitride (30–40 vol%) the grain size is decreased to about 5 μm. In this case, the shape of grains is more uniform and spherical particles are dominant. The amount of observed ceramic agglomerates is raising.

The composite powders were consolidated using a hot-pressing method in vacuum (10^{-3} Tr) at 600°C and the pressure of 415 MPa for 30 min.

The microstructure and thermal properties of the fabricated Cu-AlN composites were evaluated. The densities of composites were measured by the Archimedes method. The obtained results were compared with theoretical densities estimated from the rule of mixtures. The microstructure of Cu-AlN composites was examined using scanning electron microscopy (SEM).

The thermal expansion coefficient was measured using a vertical direct dilatometer. The samples were heated up to the temperature of 600°C in a protective argon atmosphere at a rate of 5° C/min, maintained at this temperature for 5 min and, then, cooled down in an oven at an average rate of 2 to 3°C/min. The values of the thermal expansion coefficient were determined based on the measurements of the elongation of the samples as a function of the temperature, using the equation:

$$\alpha = \frac{\Delta l}{l_0 \cdot \Delta T}, \tag{1}$$

where $\Delta l/\Delta T$ – the rate of change of the linear dimension per unit change in temperature, l_0 – initial length of the sample.

The thermal diffusivity D was measured at room temperature by a laser flash method (LFA 457, Netzsch). The front face of the measured sample was homogeneously heated by an unfocused laser pulse. On the rear face of the sample the temperature increase was measured as a function of time. The mathematical analysis of this temperature/time function allows the determination of the thermal diffusivity D. For adiabatic conditions, the diffusivity can be calculated from the following equation [18]:

$$D = 0.1388 \cdot \frac{l^2}{t_{0.5}}, \tag{2}$$

where D – diffusivity in mm^2/s, l – sample thickness in mm, $t_{0.5}$ – time at 50% of the temperature increase, measured at the rear side of the sample in s.

The specific heat was evaluated for each composition based on the rule of mixture.

The experimental results of the thermal diffusivity and calculated values of the specific heat were used to estimate the thermal conductivity K. It can be determined from the relation:

$$K = \rho \cdot c_p \cdot D, \tag{3}$$

where K – thermal conductivity in W/mK, ρ – density in g/cm^3, c_p – specific heat in J/gK, D – diffusivity in mm^2/s.

3. Results and discussion

3.1. Measurements of thermal properties. Theoretical density of the composites was defined for the assumed volume contents, using the density of aluminium nitride $\rho_{\mathrm{AlN}} = 3.20$ g/cm^3 and the density of copper $\rho_{\mathrm{Cu}} = 8.96$ g/cm^3. Table 1 shows the densities of the produced hot-pressed Cu-AlN composite materials.

Table 1
Densities of hot-pressed Cu-AlN composites

Chemical composition (vol.%)	Theoretical density (g/cm^3)	Measured density (g/cm^3)	Relative density (%)
90Cu-10AlN	8.38	8.27	98.6
80Cu-20AlN	7.81	7.69	98.4
70Cu-30AlN	7.23	7.08	97.9
60Cu-40AlN	6.66	6.45	96.9

The hot-pressed Cu-AlN composites demonstrate a good densification as confirmed by the data of density measurements. Relative densities exceed 96% in all examined cases. It can be stated that the greater volume fraction of aluminium nitride, the lower density of composite materials. Due to a higher sintering temperature of AlN (over 1600°C [19]), the degree of densification between ceramic particles is not high and, therefore, porosity appears. The hot pressing process is conducted at a much lower temperature than in the case of the AlN sintering process, but a particularly high pressure used ensures continuation of the densification process. At the temperature of 600°C copper exhibits good plasticity. That is why, we can presume that hard ceramic particles are pressed into the plastic copper matrix.

The behaviour of composite elements at the grain boundaries was investigated using scanning electron microscopy. The examples of Cu-AlN composite materials are presented in Fig. 3.

The SEM observations did not show the presence of porosity at the interface of the copper/aluminium nitride grain boundary. However, in few cases some cracks and discontinuity of the structure were found (Fig. 3b). The porosity of composite materials is, in most cases, located between ceramic grains (Fig. 3a). Their amount is raising with the increase of the ceramic phase content. It appears that the main densification mechanism is that of the diffusion of copper towards ceramic grains and plastic deformations of copper particles during the sintering process.

The major drawback of pure copper is a particularly high value of the thermal expansion coefficient (16.8×10^{-6} 1/K). The mismatch between copper and semiconductor materials can be tailored by changing the aluminum nitride volume fraction. Figure 4 shows the results of thermal expansion coefficient measurements for different Cu-AlN composite composition at room temperature.

a)

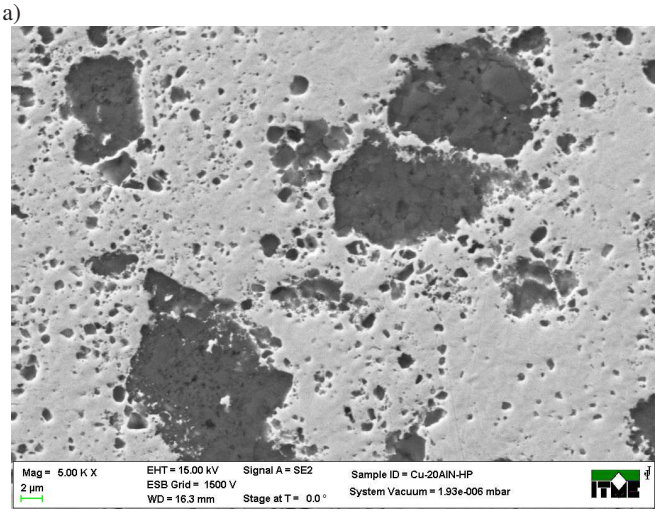

b)

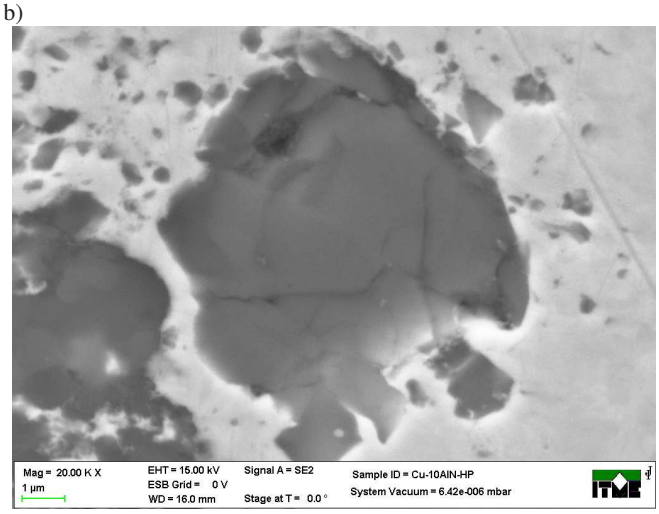

Fig. 3. SEM images of example composites obtained by hot pressing method: a) 80Cu-20AlN, b) 70Cu-10AlN

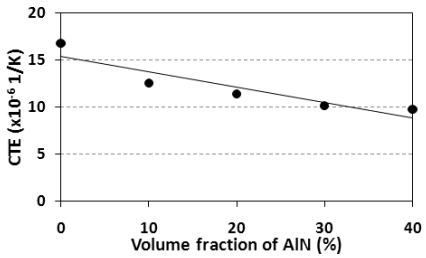

Fig. 4. Thermal expansion coefficient (at room temperature) for hot pressed Cu-AlN composite materials

The values of the thermal expansion coefficient were determined in the form of the average coefficients α_{T0-T1}, which are most often used. These coefficients describe the average thermal expansion of the material within the temperature range from the initial temperature T_0 (usually 0°C or 20°C) to the upper temperature limit T_1. For each sample, the initial temperature was $T_0 = 20$°C, whereas the temperature limit was 50, 75, 100, 125, …, 600°C. The calculated values of these coefficients (determined according to the procedure described below) are presented as diagrams in Fig. 5 and discussed with reference to the results.

a)

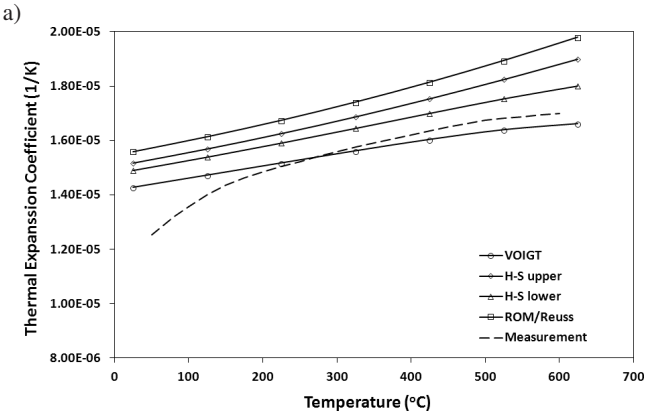

b)

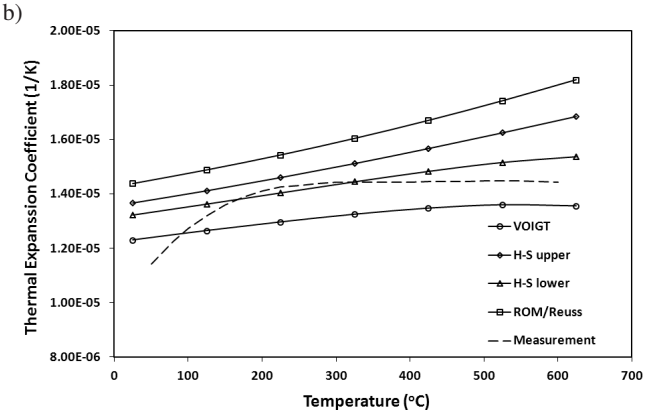

c)

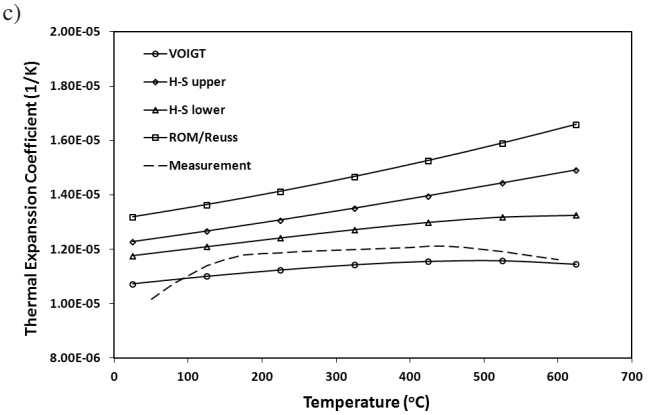

d)

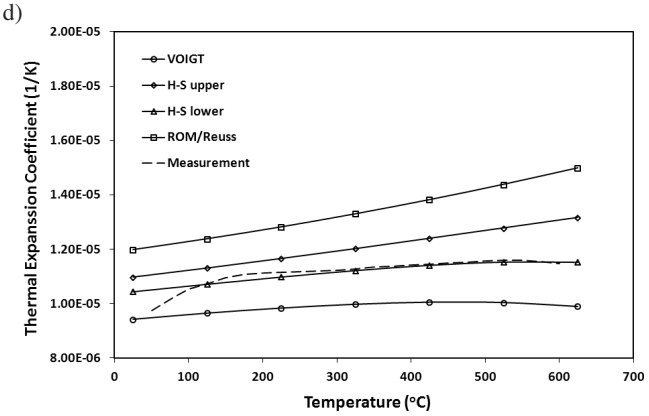

Fig. 5. Comparison of the calculated and measured coefficients of thermal expansion for different ceramic phase content: a) 10% AlN, b) 20% AlN c) 30% of AlN d) 40% of AlN (solid lines – analytical models, dashed lines – measured CTE)

It can be seen that the addition of ceramic phase caused the decrease of the thermal expansion coefficient of Cu-AlN composites, when compared to pure copper. This effect was better visible once the ceramic phase content was increased. The results of the measurements do not significantly differ from the analytical estimates furnished by the rule of mixture. The mismatch appears due to the presence of a third phase (pores) in the composite material.

The results of the measured thermal diffusivity and, thus, the thermal conductivity of the obtained composite materials are presented in Table 2.

Table 2
Results of thermal diffusivity and thermal conductivity of Cu-AlN composite materials at 50°C

Chemical composition (vol.%)	Thermal diffusivity D (mm^2/s)	Thermal conductivity K (W/mK)
90Cu-10AlN	91.75	304.45
80Cu-20AlN	74.85	238.75
70Cu-30AlN	71.62	223.36
60Cu-40AlN	54.94	164.40

For all the examined samples, the thermal conductivity turned out to be lower than expected from the properties of the constituent materials (rule of mixtures). The composite with the highest copper content (90%) had the highest thermal conductivity (slightly above 300 W/mK). As could be expected, the thermal conductivity of composites decreased with the increasing ceramic content. However, this drop was greater than that resulting from the calculations. This adverse effect can be explained by the increased porosity of the composite, which has an essential effect on the thermal conductivity since the pores present between non-sintered ceramic grains constitute a barrier to heat transfer.

3.2. Modelling of Cu-AlN thermal properties. The modelling of the thermal properties of composites is of great interest in many heat transfer applications. Two types of models of the thermal properties of a material, namely analytical and numerical [20], are present in the literature. Usually, the Voigt and Reuss bounds [21] and the Hashin-Shtrikman bounds [22–24] are used for-preliminary and fast verification of the produced composites. A number of other theoretical models such as Turner model [25], Kernel model [26], Maxwell-Eucken model or the Effective Medium Theory [27] are reported in the professional literature. When the reinforcement of a particular composite material takes the form of spherical particles or fibers the numerical modeling is commonly applied [28, 29].

In this paper we decided to use the classical Voigt-Reuss and Hashin-Shtrikman bounds for a fast evaluation of the quality of the composite, and to subsequently build up a more precise numerical model enabling the investigation of the influence of the residual porosity on the material's properties. The experimental data of the effective coefficient of thermal expansion and the thermal conductivity will be compared with the coefficient obtained from the analytical and numerical models. The following two FE material models were implemented: (i) an ideal material with no residual porosity, and (ii) a porous material where the finite element mesh was modified to allow for a third component (pores).

The roughest estimates of the effective material properties but, at the same time, the most widely used ones, are the Voigt and Reuss bounds. The Voigt upper bound is derived under the assumption of uniform stress distribution, whereas the Reuss lower bound under the assumption of uniform strain distribution. This leads to the solution of elasticity equations, where the stiffness tensor is equal to the average values of the matrix and inclusions stiffness tensors, while the compliance tensor is equal to the average values of the matrix and inclusions compliance tensors. The Voigt and Reuss bounds can be expressed as [30]:

$$\begin{aligned} \alpha_V &= \frac{f_1 E_1 \alpha_1 + f_2 E_2 \alpha_2}{f_1 E_1 + f_2 E_2}, \\ \alpha_R &= f_1 \alpha_2 + f_1 \alpha_2, \end{aligned} \tag{4}$$

where f – the volume fraction, α – the coefficient of thermal expansion, E – the Young's modulus, indices *1* and *2* denote copper and aluminium nitride phase, respectively. The Voigt and Reuss bounds of the thermal conductivity take the following form [29]:

$$\begin{aligned} k_V &= f_1 k_1 + f_2 k_2, \\ k_R &= \frac{k_1 k_2}{f_1 k_2 + f_2 k_1}. \end{aligned} \tag{5}$$

The bounds derived by Hashin and Shtrikman [22, 23] provide a very good prediction of the experimental data. Originally, they suggested analytical equations for the calculation of the bulk and shear modulus. For computing the effective thermal properties of a composite the effective elastic constants calculated from the Hashin-Shtrikman model are used to solve the elasticity equations. This leads to the following equation for the upper and lower value of the effective coefficient of thermal expansion:

$$\begin{aligned} \alpha^u &= \alpha_1 - \frac{(\alpha_1 - \alpha_2) K_2 (3K_1 + 4G_1) f_2}{K_1(3K_2 + 4G_1) + 4(K_2 - K_1) G_1 f_2}, \\ \alpha^l &= \alpha_2 - \frac{(\alpha_2 - \alpha_1) K_1 (3K_2 + 4G_1) f_1}{K_2(3K_1 + 4G_2) + 4(K_1 - K_2) G_2 f_1}, \end{aligned} \tag{6}$$

where K and G – bulk and shear modulus respectively, and the effective thermal conductivity (Eq. (7)) [23]:

$$\begin{aligned} k^u &= f_1 k_1 + f_2 k_2 - \frac{f_1 f_2 (k_1 - k_2)^2}{3k_1 - f_1(k_1 - k_2)}, \\ k^l &= f_1 k_1 + f_2 k_2 - \frac{f_1 f_2 (k_1 - k_2)^2}{3k_2 + f_2(k_1 - k_2)}. \end{aligned} \tag{7}$$

The coefficients of thermal expansion calculated from those analytical models were used for the first verification of the experimental data. In the present study, it is assumed that elastic moduli of Cu and AlN are constant, irrespective of the temperature. The values of Young's, bulk and shear moduli as well as Poisson's ratio are given in Table 3. On the other hand, the coefficients of thermal expansion of Cu and AlN are regarded as temperature dependent parameters (cf. Table 4).

Table 3
Elastic modulus of Cu and AlN

Material	Young modulus (GPa)	Bulk modulus (GPa)	Shear modulus (GPa)	Poisson ratio
AlN	310	172	129	0.21
Cu	130	72.5	54.3	0.35

Table 4
Coefficient of thermal expansion for Cu and AlN

T (°C)	25	125	225	325	425	525	625	725	825
AlN ($\times 10^{-6}$ 1/K)	4.8	4.9	5	5.1	5.2	5.3	5.4	5.5	5.6
Cu ($\times 10^{-6}$ 1/K)	16.79	17.39	18.05	18.78	19.58	20.45	21.39	22.4	23.49

A comparison of the analytical estimates and the measured coefficient of thermal expansion values for different contents of AlN is depicted in Fig. 5.

The measured coefficients of thermal expansion for all the considered contents of AlN fall between the analytical bounds. For lower temperature, the experimental data are below the Voigt lower bound due to the measurement device inaccuracy at a lower temperature range. The existing porosity has only a small effect on the value of coefficients of thermal expansion because of the real composition of the composite, which differs from the theoretical one. The large CTE of the air (about 3.5e-3 1/K) which fills the pores cannot lead to the increase of the composite's CTE because the air thermal expansion is blocked by the pores' walls.

The values of the thermal conductivity used for the calculation were as follows: 398 W/mK and 120 W/mK for copper and aluminium nitride, respectively. It was assumed that the pores are filled with air (assumed thermal conductivity of air was 0.0257 W/mK). Here, the influence of residual porosity is much more pronounced than for the thermal expansion - the measured data fell below analytical predictions for the whole range of AlN contents.

A FEM model using a academic program FEAP ver. 7.5 was developed. Two FE meshes were implemented: (i) without porosity to provide control calculations of the thermal conductivity and to make comparison with the analytical models, and (ii) with different porosities for different composites (cf. Table 1). In both cases a finite element mesh was generated as voxels of AlN randomly immersed in the copper matrix [30]. The numerical representation of the specimen (unit cell) is presented in Fig. 6.

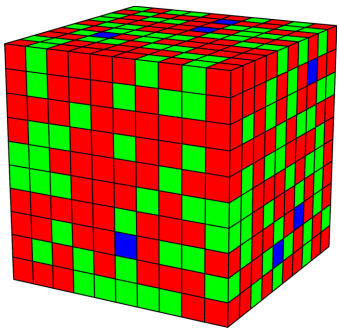

Fig. 6. The example of FE unit cell used in the modelling (gray elements represent copper, white – aluminium nitride, and black – pores)

Hexagonal, 8-nodes thermal elements which solve the linear Fourier heat conduction equation in a three-dimensional domain were used (Eq. (8)):

$$q = -k_{eff}\Delta T, \tag{8}$$

where q – thermal flux, k_{eff} – effective thermal conductivity and $\Delta T = T_{hot} - T_{cold}$.

The temperature on the two opposite faces of the specimen was constant but one face was set as hot ($T_{hot} = 100$), the opposite face was kept cold ($T_{cold} = 0$), whereas the remaining ones were assumed to be adiabatic. Following Floury at al. [31] the effective thermal conductivity was described by Eq. (9):

$$k_{eff} = -\frac{Q_1}{A}\frac{L}{(T^1_{hot} - T^1_{cold})}, \tag{9}$$

where L – the length of the unit cell side, A – the cross-section area of the unit cell ($A = L^2$), $T^1_{hot} - T^1_{cold}$ – the temperature difference across the unit cell, Q_1 – the overall heat flux into the unit cell obtained by integrating fluxes across the inlet face of unit cells (Eq. (10)):

$$Q_1 = \int_A -k\frac{\partial T}{\partial z}dxdy. \tag{10}$$

The above equation was used for all unit cells in order to calculate the thermal flux and the effective thermal conductivity. The results obtained from the FE model with and without porosity are presented in Fig. 7.

The mesh without porosity was applied to verify if the implementation of the thermal conductivity model was successful. The results derived from it should lie between the Hashin-Shtrikman bounds. As one can see, the results from the numerical modelling for the no-porosity case lie exactly between the bounds (triangles in Fig. 7). The next step was the implementation of the FE mesh with the residual porosity. Using the data from Table 1, the porosity equals 1.4%, 1.6%, 2.1% and 3.1% for the AlN content of 10%, 20%, 30% and 40%, respectively. Material porosity results in a substantial decrease of the thermal conductivity, which is much larger than for an ideal material (diamond symbols in Fig. 7). The numerical results are close to the experimental data for all AlN contents.

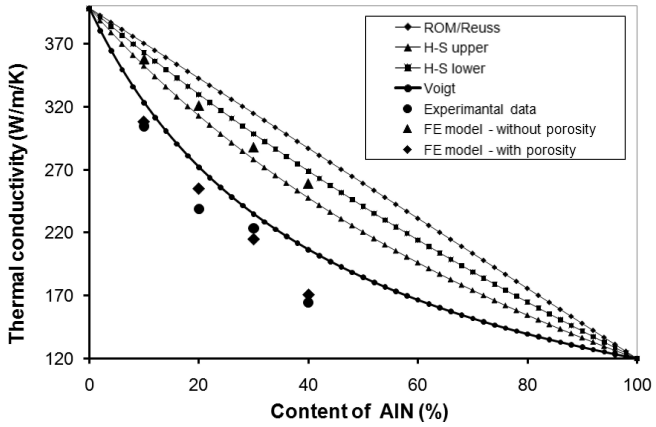

Fig. 7. Comparison of the calculated (analytically and numerically) and measured thermal conductivity for different ceramic phase contents

This simple numerical model can also be employed to provide reliable approximations of thermal properties of composites with different compositions. It can help materials design engineers to assess the influence of the porosity in a particular composite material prior to its processing.

4. Conclusions

The paper presents results of experimental and modeling studies concerning thermal properties of the Cu-AlN composite materials, which are of crucial importance when they are to be used in heat-dissipating systems. The technological conditions allowing to obtain almost fully dense composite materials were elaborated using hot pressing method. The increase of porosity with the raise of ceramic volume content in the composite was observed. The increasing porosity of these composites was the principal reason why their thermal conductivity is lower than expected. Some cracks observed in the composite structure have also negative influence on their thermal properties. Comparing the previous results of other authors [32] obtained results are very promising in the electronic applications.

From the presented analytical and numerical models it can be concluded that the residual porosity has a minor influence on the coefficients of thermal expansion values but leads to a large decrease of the thermal conductivity of a composite, especially when compared to an ideal material (without porosity). A good prediction of the thermal conductivity was obtained from the FE model of a material with residual porosity. The difference between the results obtained from the model and the experimental data does not exceed 5%. The proposed numerical model can be easily extended to predict the thermal properties of other composites, and can, thus, be helpful in the composite materials design.

Acknowledgements. This work was supported by the Polish Ministry of Science and Higher Education (the project No N508 3086 33).

REFERENCES

[1] D.D.L. Chung, "Materials for thermal conduction", *Applied Thermal Engineering* 21, 1593–1605 (2001).

[2] J. Korab, P. Stefanik, S. Kavecky, P. Sebo, and G. Korb, "Thermal conductivity of undirectial copper matrix carbon fibre composites", *Composites* A 33, 577–581 (2002).

[3] A. Brendel, C. Popescu, C. Leyens, J. Woltersdorf, E. Pippel, and H. Bolt, "SiC-fiber reinforced copper as heat-sink material for fusion applications", *J. Nuclear Materials* 329–333, 804–808 (2004).

[4] V.K. Lindroos and M.J. Talvitie, "Recent advances in metal matrix composites", *J. Materials Processing Technology* 53, 273–284 (1995).

[5] K. Hanada, K. Matsuzaki, and T. Sano, "Thermal properties of diamond particle-dispersed Cu composites", *J. Materials Processing Technology* 153–154, 514–518 (2004).

[6] K. Yoshida and H. Morigami, "Thermal properties of diamond/copper composite material", *Microelectronics Reliability* 44, 303–308 (2004).

[7] F. Boey, A.I.Y. Tok, Y.C. Lam, and S.Y. Chew, "On the effects of secondary phase on thermal conductivity of AlN ceramic substrates using a microstructural modeling approach", *Materials Science Engineering* A 335, 281–289 (2002).

[8] J. Tian and K. Shobu, "Hot-pressed AlN-Cu metal matrix composites and their thermal properties", *J Materials Science* 39, 1309–1313 (2004).

[9] M. Barlak, W. Olesinska, J. Piekoszewski, M. Chmielewski, J. Jagielski, D. Kalinski, Z. Werner, and B. Sartowska, "Ion implantation as a pre-treatment method of AlN substrate for direct bonding with copper", *Vacuum* 78, 205–209 (2005).

[10] W. Olesinska, D. Kalinski, M. Chmielewski, R. Diduszko, and W. Wlosinski, "Influence of titanium on the formation of a "barrier" layer during joining an AlN ceramic with copper by the CDB technique", *J. Materials Science: Materials in Electronics* 17 (10), 781–788 (2006).

[11] J. Piekoszewski, W. Olesinska, J. Jagielski, D. Kalinski, M. Chmielewski, Z. Werner, M. Barlak, and W. Szymczyk, "Ion implanted nanolayers in AlN for direct bonding with copper", *Solid State Phenomena* 99–100, 231–234 (2004).

[12] M. Barlak, W. Olesinska, J. Piekoszewski, Z. Werner, M. Chmielewski, J. Jagielski, D. Kalinski, B. Sartowska, and K. Borkowska, "Ion beam modification of ceramic component prior to formation of AlN-Cu joints by direct bonding process", *Surface & Coatings Technology* 201, 8317–8321 (2007).

[13] Z. Lindemann, K. Skalski, W. Wlosinski, and J. Zimmerman, "Thermo-mechanical phenomena in the process of friction welding of corundum ceramics and aluminium", *Bull. Pol. Ac.: Tech.* 54 (1), 1–8 (2006).

[14] J. Songzhe, Z. Hailong, L. Jing-Feng, and J. Shusheng, "TiB_2-AlN-Cu functionally graded materials (FGMs) fabricated by spark plasma sintering (SPS) method", *Key Engineering Materials* 280–283, 1881–1884 (2005).

[15] W. Weglewski, M. Basista, M. Chmielewski, and K. Pietrzak, "Modelling of thermally induced damage in the processing of Cr-Al_2O_3 composites", *Composites* B 43 (2), 255–264 (2012).

[16] M. Chmielewski, D. Kalinski, K. Pietrzak, and W. Wlosinski, "Relationship between mixing conditions and properties of sintered 20AlN/80Cu composite materials", *Archives of Metallurgy and Materials* 55 (2), 579–585 (2010).

[17] D. Kalinski, M. Chmielewski, K. Pietrzak, and K. Choregiewicz, "An influence of mechanical mixing and hot-pressing on properties of NiAl/Al_2O_3 composite", *Archives of Metallurgy and Materials* 57 (3), 694–702 (2012).

[18] S. Min, J. Blumm, and A. Lindemann, "A new laser flash method for measurement of the thermophysical properties", *Thermochimica Acta* 455, 46–49 (2007).

[19] L.Ran-Rong, "Development of high thermal conductivity aluminum nitride ceramic", *J. American Ceramic Society* 74, 2242–49 (1991).

[20] J. Wang, J.K. Carson, M.F. North, and D.J. Cleland, "A new approach to modelling the effective thermal conductivity of heterogeneous materials", *Int. J. Heat and Mass Transfer* 49, 3075–3083 (2006).

[21] J. Mihans, S. Ahzi, H. Garmestani, M.A. Khaleel, X. Sun, and B.J. Koeppel, "Modeling of the effective elastic and thermal properties of glass-ceramic solid oxide fuel cell seal materials", *Materials and Design* 30, 1667–1673 (2009)

[22] Z. Hashin and S. Shtrikman, "A variational approach to the theory of the elastic behaviour of polycrystals", *J. Mechanics and Physics of Solids* 10, 343352 (1962)

[23] Z. Hashin and S. Shtrikman, "A variational approach to the theory of the elastic behaviour of multiphase materials", *J. Mechanics and Physics of Solids* 11, 127–150 (1963)

[24] J. Wang, B.L. Karihaloo, and H.L. Duan, "Nano-mechanics or how to extend continuum mechanics to nano-scale", *Bull. Pol. Ac.: Tech.* 55 (2), 133–140 (2007).

[25] P.S. Turner, "Thermal expansion stresses in reinforced plastics", *J. Research National Bureau of Standards* 37, 239–60 (1946).

[26] E.H. Kerner, "The elastic and thermo-elastic properties of composite media", *Proc Physics Society Section* B 69 (8), 808813 (1956).

[27] G. Buonanno and A. Carotenuto, "The effective thermal conductivity of packed beds of spheres for a finite area", *Numerical Heat Transfer, Part A: Applications* A 37 (4), 343–357 (2000).

[28] R.P.A. Rocha and M.E. Cruz, "Computation of the effective conductivity of unidirectional fibrous composites with an interfacial thermal resistance", *Numerical Heat Transfer, Part A: Applications* A 39 (2), 179–203 (2001).

[29] W. Pabst and E. Gregorova, "Effective thermal and thermoelastic properties of alumina, zirconia and alumina–zirconia composite ceramics", in *New Developments in Materials Science Research*, ed. B.M. Caruta, pp. 77–137, Nova Science Publishers, New York, 2009.

[30] W. Weglewski, M. Chmielewski, D. Kalinski, K. Pietrzak, and M. Basista, "Thermal residual stresses generated during processing of Cr/Al_2O_3 composites and their influence on macroscopic elastic properties", *Advances in Science and Technology* 65, 27–32, (2010).

[31] J. Floury, J. Carson, and Q. Tuan Pham, "Modelling thermal conductivity in heterogeneous media with the finite element method", *Food and Bioprocess Technology* 1, 161–170 (2008).

[32] L. Kwang-Min, O. Dae-Keun, C. Woong-Sub, T. Weissgarber, and B. Kieback, "Thermomechanical properties of AlN-Cu composite materials by solid state processing", *J. Alloys and Compounds* 434–435, 375–377 (2007).